EARTH SURFACE PROCESSES AND LANDFORMS, VOL 22, 195–209 (1997)

COSMOGENIC ISOTOPE ANALYSES APPLIED TO RIVER LONGITUDINAL PROFILE EVOLUTION: PROBLEMS AND INTERPRETATIONS

MICHELE A. SEIDL,[1]*ROBERT C. FINKEL,[2] MARC W. CAFFEE,[2] G. BRYANT HUDSON[2] AND WILLIAM E. DIETRICH[3]

[1]*Department of Geological Sciences, Rutgers University, New Brunswick, NJ 08903, USA*
[2]*Lawrence Livermore National Laboratory, Livermore, CA 94550, USA*
[3]*Department of Geology and Geophysics, University of California at Berkeley, Berkeley, CA 94720, USA*

Received 23 July 1996; Revised 6 August 1996; Accepted 6 August 1996

ABSTRACT

The use of cosmogenic isotopes to determine surface exposure ages has grown rapidly in recent years. The extent to which cosmogenic nuclides can distinguish between mechanistic hypotheses of landscape evolution is an important issue in geomorphology. We present a case study to determine whether surface exposure dating techniques can elucidate the role knickpoint propagation plays in longitudinal profile evolution. Cosmogenically produced ^{10}Be, ^{26}Al, ^{36}Cl, ^{3}He and ^{21}Ne were measured in olivines collected from 5·2 Ma basalt flows on Kauai, Hawaii. Several obstacles had to be overcome prior to the measurement of *in situ*-produced radionuclides, including removal of meteoric ^{10}Be from the olivine grains. Discrepancies between the radionuclide and noble gas data may suggest limits for exposure dating. Approximate surface exposure ages calculated from the nuclide concentrations indicate that large boulders may remain in the Hawaiian valley below the knickpoint for hundreds of thousands of years. The ages of samples collected above the knickpoint are consistent with estimates of erosion based on the preservation of palaeosurfaces. Although the exposure ages can neither confirm nor reject the knickpoint hypothesis, boulder ages downstream of the knickpoint are consistent with a wave of incision passing upvalley. The long residence time off the coarse material in the valley bottom further suggests that knickpoint propagation beneath a boulder pile is necessary for incision of the bedrock underlying the boulders to occur.

Earth surf. processes landf., **22**, 195–209 (1997)
No. of figures: 6 No. of tables: 6 No. of refs: 41
KEY WORDS: cosmogenic isotopes; river incision; longitudinal profile development; landscape evolution

INTRODUCTION

A complete understanding of landscape evolution requires not only the elucidation of the mechanisms that modify landscapes, but also determination of the rates at which landscapes respond to tectonic and climatic signals. One of the greatest challenges in geomorphology lies in constraining these rates of landscape development. Channel incision into bedrock serves as a boundary condition to hillslope development and, as such, provides a critical link between landscape evolution and base level. Yet, the development of river longitudinal profiles into bedrock remains poorly understood. Studies of bedrock fluvial systems indicate that more than one transport law is necessary to characterize river incision and longitudinal profile development and, similarly, that several incisional mechanisms operate along bedrock channels (Seidl and Dietrich, 1992; Howard *et al.*, 1994; Seidl *et al.*, 1994). The relative importance of these mechanisms in the evolution of river profiles, as well as the relative rates of landscape lowering associated with them, is not well known.

Since the seminal work of Kurz (1986a, b) and Craig and Poreda (1986), the use of cosmogenic isotope analyses in geomorphology has allowed the dating of exposed surfaces and the establishment of timing in many Quaternary landscapes (for recent reviews, see Cerling and Craig (1994) and Bierman (1994)). The question we

* Correspondence to: M. A. Seidl
Contract grant sponsor: LLNL-IGPP; contract grant numbers: 92–10 and 93–34.
Contract grant sponsor: DOE; contract grant number: W-7405-Eng-48.

CCC 0197-9337/97/030195–15

can now ask is do we have the resolution, using these techniques, to test models of landscape development? This issue is currently being addressed using a range of cosmogenic nuclides because these data can be used both to calculate exposure ages and to assess the rate of erosion acting upon the surfaces (Nishiizumi *et al.*, 1991; Lal, 1991). Recently, ^{10}Be and ^{26}Al concentrations have been analysed in surficial processes, tectonics and climate change studies. ^{10}Be concentrations measured in soil samples have been used both to quantify soil production rates and provide evidence for a linear diffusion model of hillslope development (McKean *et al.*, 1993; Monaghan *et al.*, 1992). Slip rates have been determined along active faults and earthquake recurrence intervals have been estimated using cosmogenic data and models (Ritz *et al.*, 1995; Bierman *et al.*, 1995). The development of soils and laterite formation have been investigated using cosmogenic nuclides (Brown *et al.*, 1994) and ^{10}Be data have been used to constrain the timing of glacial advance and retreat (Phillips *et al.*, 1990; Gosse *et al.*, 1995). Exposure ages have been calculated for surface samples to investigate the climate history of the Dry Valleys region of the Transantarctic Mountains since the Pliocene (Ivy-Ochs *et al.*, 1995). Burbank *et al.*, (1996) have dated strath terraces to estimate bedrock erosion rates in the rapidly uplifting Himalayas. Several authors have reported the measurement of radionuclide concentrations in sediments; the data are used to estimate basin-wide mean denudation rates (e.g. Granger *et al.*, 1996; Bierman and Steig, 1996; Brown and Gangue, 1995).

This paper presents an effort to link a field-based study with surface exposure dating techniques to understand river longitudinal profile evolution. The study was aimed at improving our understanding of the rates and processes governing bedrock channel incision. Samples to be analysed for cosmogenic isotopes were collected along a river profile and both radionuclide and stable nuclide concentrations were measured in the rocks. Measurement of cosmogenic isotope concentrations, specifically the nuclides ^{10}Be, ^{26}Al, ^{36}Cl, ^{21}Ne and ^{3}He, allows direct quantification of exposure ages and erosion rates and permits quantitative assessment of the processes operating in the studied landscape.

The ubiquity of olivine-rich basalts precluded the use of quartz in our work. Following Kurtz (1986a, b), we intended to analyse the noble gas content of olivines in our surface exposure age dating study. We then expanded the scope of the study and measured radionuclide concentrations in the olivines. In contrast to the numerous studies utilising quartz, olivine is much more seldom used for radionuclide work (Nishiizumi *et al.*, 1990; Shepard *et al.*, 1995) because of its variable chemical composition, its high aluminium content and the difficulty of removing meteoric ^{10}Be. As will be seen below, olivines imposed several experimental difficulties which limited the strength of the conclusions we could reach, but which indicated that olivines do have some promise for further work. Our study included the measurement of multiple isotopes in single olivine samples. Comparison of these data has implications both for the processes attending river development and isotope systematics.

BACKGROUND: KAUAI CHANNELS

We focused our study on the Hawaiian island of Kauai. Kauai is an ideal area in which to analyse longitudinal profile evolution using cosmogenic isotopes because: (1) longitudinal profile forms are known; (2) channel and hillslope forms are repeated on adjacent Kauai watersheds of similar age and lithology and with similar base level and climate histories; (3) these morphologies have been linked to the different boundary conditions under which the channels developed; (4) two distinct incisional processes have been identified as operating on the channels – vertical lowering of the channel bed by abrasion and dissolution processes, and stepwise lowering by knickpoint propagation; (5) quantitative estimates of the erosion rates associated with both knickpoint retreat and vertical lowering have been made; and (6) lava flows are olivine-rich, so material is available for cosmogenic isotope analyses (Seidl *et al.*, 1994). The Kauai landscape provides a well-constrained framework in which to assess surface exposure ages.

The Kauai channels flow across western Kauai and are incised into gently dipping, 5·2 Ma basalt flows (Figure 1) (Clague and Dalrymple, 1987). Long-term erosion rates can be estimated along the river profiles based on the 5·2 Ma age of the flows and the preservation of ridges above the channels that are considered to be equivalent to the initial lava flow surfaces (Seidl *et al.*, 1994). The longitudinal profiles of the channels are either straight or punctuated by distinct convexities, or knickpoints. The convex channels drain to the Napali Coast

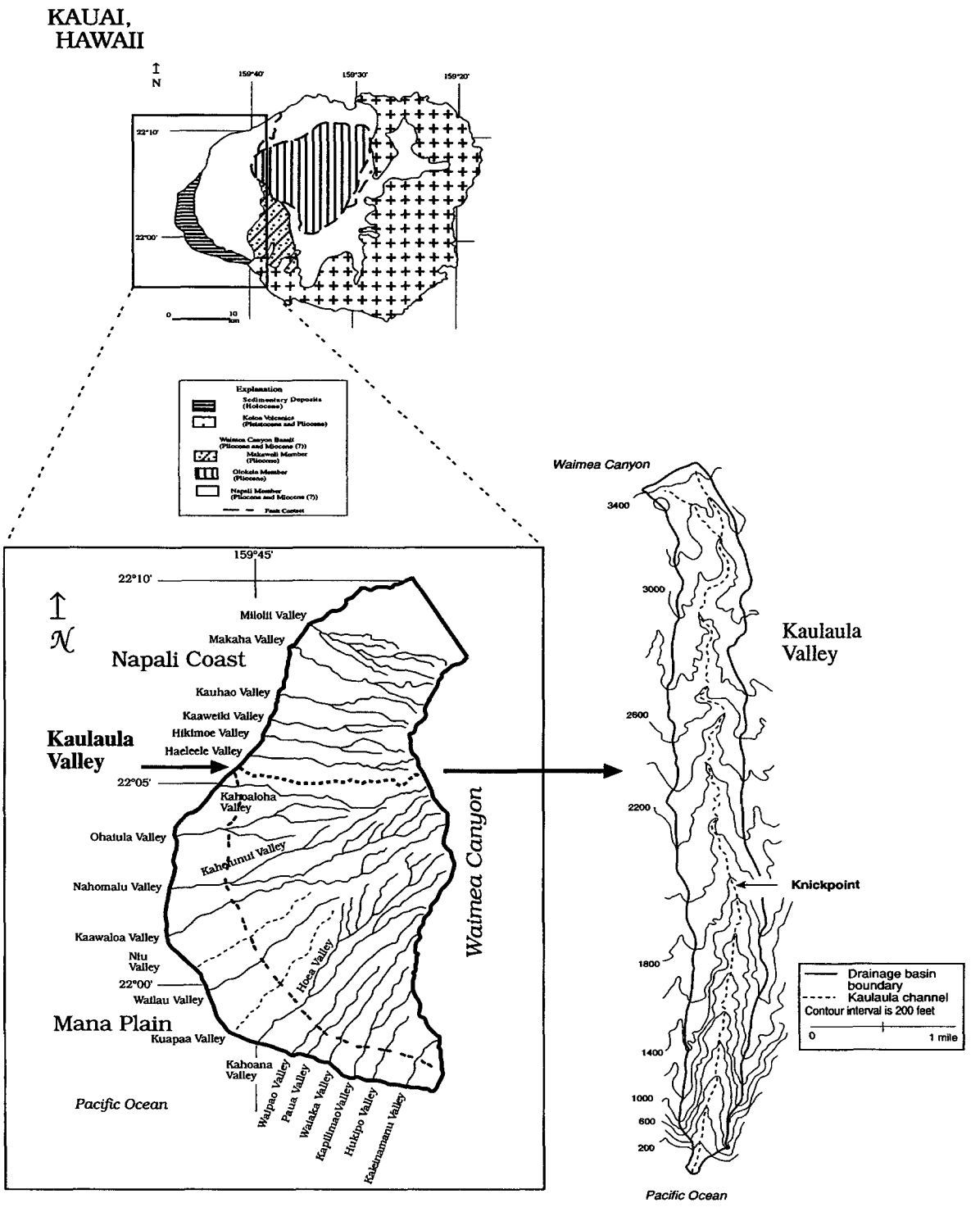

Figure 1. Map delineating general geology of Kauai (modified from Stearns (1985) and Seidl *et al.* (1994)) and detail of Napali Coast and Mana Plain basins. Kaulaula Valley, the focus of the sampling, is highlighted by an arrow, and the topography of Kaulaula Valley, digitized from 7·5′ topographic map, is shown.

and are located to the north of the generally straight channels, which drain to the sea out and across the Mana Plain (Figure 1) (Seidl *et al.*, 1994). These differences in profile form have been linked to the different base level histories of the Napali Coast and Mana Plain channels, and suggest that knickpoint propagation is important in channel erosion of bedrock under conditions of rapid base level change (Seidl *et al.*, 1994). Evidence for knickpoint propagation can also be found by examining hillslope morphologies upstream and downstream of the convexities within a basin. Upstream of the knickpoints, valley walls are soil-mantled and typically have gentle gradients. In contrast, valley walls downstream of the knickpoints are steep and lack soil cover, and the V-shaped valley is deeply incised. The different valley forms have been associated with a change in the process of incision across the knickpoint (Seidl *et al.*, 1994). The channel reaches extending upstream of the knickpoints appear to be dominated by abrasion and dissolution of the channel bed, whereas the channel reaches and valley walls extending downstream of the knickpoints appear to be formed primarily by the upstream propagation of knickpoints (Seidl *et al.*, 1994). The knickpoints are hypothesized to form at the coastline and propagate upstream. Based on the base level history of the channels and on models of coastal evolution, the knickpoints are estimated to migrate upvalley at a rate of kilometres per million years (Seidl *et al.*, 1994).

Exposure ages of samples collected along a river profile containing a distinct knickpoint should allow differentiation between (1) propagating knickpoints that originate at the coast and migrate as a consequence of rapid base level change, and (2) long-lived knickpoints influenced by bedrock properties. Most casual impressions of waterfalls are that they are formed on more resistant rock units as a consequence of lithologic variation. If so, the Kauai knickpoints may represent static features that either do not propagate or else propagate very slowly. Figure 2 shows schematically the expected trends in isotopic concentration assuming both static and migrating knickpoints. In the top panel of the figure, a characteristic Kauai basin is illustrated, with the channel profile and ridge above the channel shown. In scenario A, the knickpoint is shown to have formed by differential rates of vertical erosion. In scenario B, the channel profile has developed because the knickpoint has migrated upstream. The bottom panel shows hypothetical isotopic concentrations for samples collected upstream and downstream of the knickpoint. The dotted line (labelled A) shows isotopic concentration, and hence exposure age, increasing from the sea to the knickpoint. This pattern is consistent with formation of the knickpoint by differential rates of vertical erosion, consequent to differential bedrock resistance. Conversely, the dashed line (labelled B) shows the isotopic concentration of bedrock in the channel decreasing from the sea towards the knickpoint and remaining constant above the knickpoint. This curve corresponds to incision principally by knickpoint propagation, as shown in scenario B.

SAMPLING STRATEGY

Samples were collected along a river profile with a distinct knickpoint to test between the two hypotheses discussed above. Ten surfaces were sampled along the Kaulaula Valley, Kauai (Figure 3). Kaulaula Valley was chosen because its profile is marked by a single, discrete knickpoint located 4 km upstream and the channel is accessible (Figure 1). Figure 2 is drawn specific to Kaulaula Valley, where long-term erosion rates in the lower part of the basin decrease in the upstream direction, such that the average erosion rate at sea level is roughly twice that below the knickpoint, and average erosion rates in the upper part of the basin are low and relatively uniform, as the channel profile is straight. The flows sampled are the Napali member of the Waimea Canyon basalt (Clague and Dalrymple, 1987). The majority of samples were collected using a sledgehammer; two samples consisted of drilled cores.

Our sampling strategy was affected by the observation that large boulders mantle the channel bed downstream and upstream of the knickpoint. Consequently, both bedrock channel bed and boulders were sampled (Figure 3). Large boulders should serve as proxies for the underlying channel bedrock if they remain stationary for long periods. If knickpoints are propagating features, the boulders may have been deposited as a wave of incision swept upstream and boulder exposure ages should record at least a minimum age for knickpoint passage. Although it could be suggested that a boulder exposure age will not only record time spent on the valley floor, but also time spent on the valley wall from which it eroded, this seems very unlikely. In the field there was abundant evidence of broken and fractured basalt lying at the bases of the valley walls, which are commonly near vertical cliffs, and this breakup probably precludes retention of previous exposure signatures.

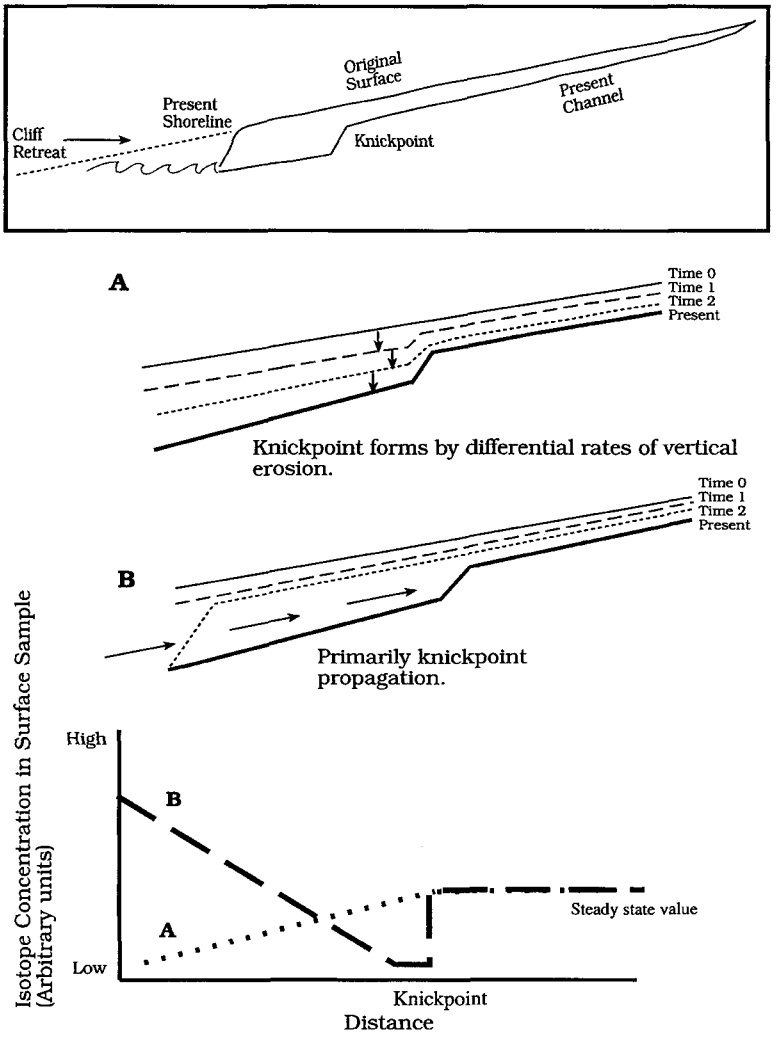

Figure 2. Hypothesized surface exposure ages along Kaulaula Valley. The top panel shows the present channel profile. In scenario A, the knickpoint is shown to form as a result of differential bedrock resistance and corresponding differential rates of vertical incision. In scenario B, the knickpoint forms at base level and propagates upstream. In the bottom panel, hypothesized isotope concentration patterns are shown in surface samples assuming different processes of knickpoint formation.

The boulders are very large, angular, often covered by a thin weathering rind, and stored on stable-appearing debris terraces adjacent to the channel. The size of the boulders implies that, unless they weather *in situ*, the only way the river can continue to cut down is to lower underneath them. Boulders appeared to be more weathered with increasing distance downstream of the knickpoint. No evidence of flood remobilization of coarse material was found in the field, which suggests that the boulders are not episodically transported. In addition, the main Kaulaula channel is at depositional grade and so precludes debris flow mobilization and scour of the main channel downstream of the knickpoint.

Five boulders were sampled downstream of the knickpoint (K560, L600, R900, L900 and R1600, shown on Figure 3). The sampled boulders were 1–3 m in diameter and were located on the upper parts of these well-defined debris terraces. The channel bedrock at the waterfall lip was sampled (KCKPD), as was a bedrock surface outcropping just downstream of the waterfall face (KKP) (Figure 3). Two kilometres upstream of the knickpoint, an alluvial terrace overlying a bedrock terrace is exposed on the right bank of the channel and the underlying strath surface was sampled (ST2040) (Figure 3). One hundred metres downstream of these terraces,

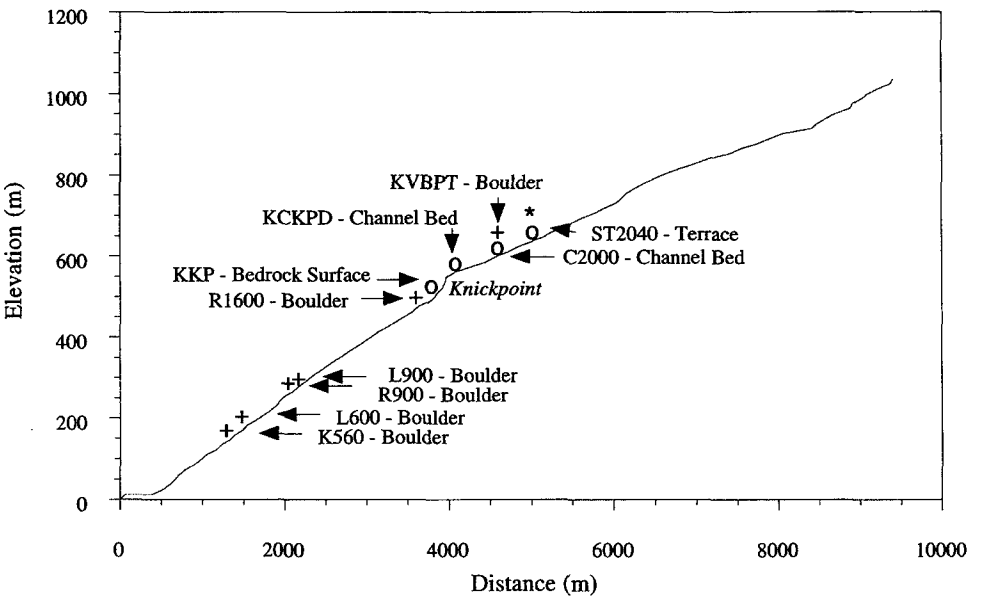

Figure 3. Sampling site locations shown on Kaulaula Valley longitudinal profile.

a boulder perched atop a pedestal of weathered bedrock was sampled (KVBPT), as was the bedrock outcropping in the channel bank (C2000) (Figure 3).

GEOCHEMICAL ANALYSIS METHODS

Whole-rock samples were crushed under water and sieved. Grains in the range from 1 to 2 mm, as well as phenocrysts larger than 2 mm, were hand-picked. Uniform grain-sized olivine phenocrysts from 1 to 0·25 mm and from 0·5 to 0·25 mm were magnetically separated. Grains smaller than 0·25 mm were not analysed. Olivine compositions were analysed using an electron microprobe; sample compositions ranged from forsterite 82 to 87 (Seidl, 1993).

Radionuclide sample preparation and measurement

Because we are interested in the *in-situ*-produced ^{10}Be, any meteoric ^{10}Be must be removed from the surfaces of the olivine crystals. Contamination by meteoric ^{10}Be is less of a problem when quartz crystals are analysed (Nishiizumi *et al.*, 1990; Kohl and Nishiizumi, 1992). Only near the end of this work did we devise a technique that effectively removed meteoric ^{10}Be, allowing isolation of the *in-situ*-produced component. We developed an etching process to remove the meteoric component, which was found to make up as much as 80 per cent of the total ^{10}Be measured. This technique was applied to olivines collected from the surface of one boulder (sample K560). After each etching step, an aliquot of the olivine crystals was removed, and both ^{10}Be and ^{26}Al concentrations were measured in each aliquot. The first sample analysed (K560A) was not subjected to any etching solution, in order to provide a baseline for the experiment. Subsequent samples, K560B–G, were leached in dilute HF and HCl solutions (Seidl, 1993). After each step, the cleaned olivines were dissolved. The resulting solutions were spiked with ^{9}Be. The high ^{27}Al content of the olivines, determined by standard addition atomic absorption spectrometry, precluded the addition of Al carrier. After separation of Be and Al by cation

and anion exchange chromatography, the high Mg content of the olivines necessitated by acetylacetone extraction (Seidl, 1993). Subsequently, BeO and Al_2O_3 were purified by solvent extractions and precipitation.

Four samples were prepared for ^{36}Cl analysis following the procedure of Zreda *et al.* (1991). The basalt samples were first ground to a fine powder (c.36–100μm) and leached with 0·1 N HNO_3 to remove the meteoric (anthropic) chlorine. The leached groundmass was then dissolved with concentrated HF and HNO_3 in a 3:1 and 1:1 ratio of acid to mass, respectively. The resulting gas was distilled to a capture tube containing a 5 per cent AgCl–HF–HNO_3 mixture. AgCl precipitated in this trap and further purification was performed with $Ba(NO_2)_3$ to reduce the amount of sulphur in the final product. The ^{35}Cl content of the basalts was determined using neutron activation analysis.

All ^{10}Be, ^{26}Al and ^{36}Cl measurements were performed by accelerator mass spectrometry (AMS) at the Center for Accelerator Mass Spectrometry, Lawrence Livermore National Laboratory, USA.

^{3}He and ^{21}Ne sample preparation and measurement

Samples for ^{3}He and ^{21}Ne analyses by noble gas mass spectrometry required no further chemical purification beyond collection of olivine mineral separates. When possible, olivine samples were crushed on-line and the gas released was measured. In all cases, the samples were melted in several heating steps in a resistance-heated furnace. Isotopic measurements were made on a VG 5400 spectrometer fitted with pulse counting. Helium and neon ratios were standardized against air. All values have been corrected for interference peaks, and extraction and instrumental blanks.

RESULTS

Radionuclide data

The ^{10}Be and ^{26}Al results from the leaching experiment are presented in Figure 4 and Table I; it is important to note that the ^{26}Al results are presented as upper limits at two standard deviations. Approximately 11 per cent of the surface material was removed over the course of the six leaches, similar to the 11 per cent loss cited by Nishiizumi *et al.* (1990). The results indicate that the number of ^{10}Be atoms decreased by a factor of five, while the number of ^{26}Al atoms remained constant during the final three etching steps. The method was used successfully to leach meteoric ^{10}Be from olivine samples collected from Lunar Crater, USA (Shepard *et al.*, 1995). Prior to the leaching experiment, several samples were analysed for ^{10}Be and ^{26}Al. These ^{26}Al data are

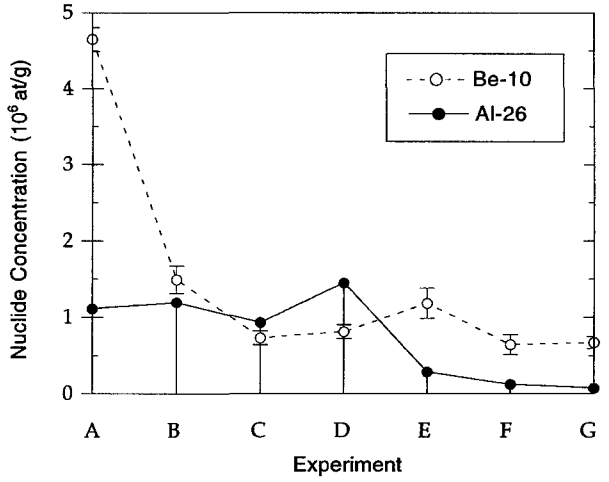

Figure 4. Results of the etching experiment in which rock aliquots were analysed both for ^{10}Be and ^{26}Al concentrations. Sample A corresponds to an unleached sample, with each successive letter denoting a more etched sample. Note: the ^{26}Al concentrations plotted are upper limits at two standard deviations.

Table I. ^{10}Be etching process data

Sample	Weight (g)	Al conc. (10^3 ppm)	^{26}Al/^{27}Al ($\times10^{-14}$)	^{26}Al* (10^6 atoms g^{-1})	Be carrier (g)	^{10}Be/^{9}Be ($\times10^{-13}$)	^{10}Be (10^6 atoms g^{-1})	^{26}Al/^{10}Be
K560A	4·89	3·85	<1·3	<1·11	0·4717	7·23	4·65 (±0·16)	0·23
K560B	4·99	1·79	<3·0	<1·19	0·5151	2·16	1·49 (±0·18)	0·80
K560C	4·92	1·89	<2·2	<0·93	0·5016	1·07	0·73 (±0·09)	1·27
K560D	5·06	1·48	<4·4	<1·45	0·5104	1·20	0·81 (±0·09)	1·79
K560E	5·28	1·27	<1·0	<0·28	0·5441	1·72	1·18 (±0·20)	0·24
K560F	7·10	0·68	<0·8	<0·12	0·5143	1·32	0·64 (±0·13)	0·19
K560G	11·10	0·55	<0·6	<0·07	0·5095	2·20	0·67 (±0·08)	0·10

*Numbers are upper limits at two standard deviations

Table II. ^{26}Al Data

Sample	Weight (g)	Al concentration (10^3 ppm)	^{26}Al/^{27}Al	^{26}Al* (10^6 atoms g^{-1})
K560A–G (see Table I)				
L600	5·08	2·75	$7·76\times10^{-15}$	0·47 (±0·12)
R900	10·01	3·93	$<2·7\times10^{-16}$	<0·02
L900-T	5·14	6·27	$<3·6\times10^{-15}$	<0·50
L900-S	5·16	5·19	$<3·6\times10^{-15}$	<0·42
R1600	10·15	7·34	$<1·7\times10^{-15}$	<0·28
KKP1	4·98	1·68	$<3·0\times10^{-15}$	<0·11
KVBPT	8·75	3·66	$<1·5\times10^{-14}$	<1·23
KCKPD	3·09	9·76	$<1·6\times10^{-15}$	<0·35
C2000	5·51	10·96	$<5·9\times10^{-15}$	<1·44

*Unless otherwise noted, numbers are upper limits at two standard deviations

presented in Table II. The ^{10}Be results are not reported, as the concetrations include both meteoric and *in-situ*-produced ^{10}Be.

We calculate a maximum ^{26}Al/^{10}Be ratio of 2·2 for sample K560 using the upper limit ^{26}Al data and the final ^{10}Be concentration of $0·67\times10^6$ atoms g^{-1}. Nishiizumi *et al.* (1990) report an observed ^{26}Al/^{10}Be ratio of 2·6(±0·9) in Maui olivines, which agrees well with the expected value of 2·9 based on production rate calculations for olivine of known composition.

A surface exposure age was calculated for sample K560 based on the final ^{10}Be leaching experiment datum, and maximum surface exposure ages were calculated from the ^{26}Al data, all assuming production rates based on Nishiizumi *et al.* (1989). Olivine compositional variations were taken into account when calculating the ^{10}Be and ^{26}Al production rates. All ages were corrected for sample latitude and altitude according to the polynomials published in Lal (1991). Canopy cover was assumed to have negligible shielding effect. Where necessary, exposure ages were corrected for exposure geometry. Boulder ages, in general, increase with decreasing size, consistent with weathering *in situ*, such that boulders on the order of 1 m in diameter are older than those 2 m in diameter.

The ^{36}Cl data are presented in Table III. Production rates were based on Zreda *et al.* (1993) and were corrected for sample altitude and latitude (Lal, 1988).

Table III. ^{36}Cl data

Sample	Cl (ppm)	^{36}Cl/Cl ($\times10^{-13}$)
K560	36 (±2)	8·08 (±0·23)
KVBPT	45 (±4)	10·8 (±0·91)
KCKPD	58 (±2)	9·45 (±0·42)
L600	40 (±2)	9·31 (±0·50)

Table IV. ^{3}He data

Sample	Temperature step (°C)	R/R_a	^{3}He (atoms g^{-1})	^{4}He (atoms g^{-1})
K560A	crush	17·9	8·57e+05	3·42e+10
	500	0·7	2·19e+05	2·29e+11
	1700	12·3	3·94e+06	2·29e+11
	1700	12·0	1·88e+05	1·12e+10
K560B	crush	22·5	1·37e+06	4·34e+10
	500	4·8	2·27e+04	3·35e+09
	800	14·1	1·37e+06	6·93e+10
	1700	122·70	8·71e+06	9·93e+09
L600	crush	18·7	1·81e+05	6·91e+09
	crush	11·9	7·79e+04	4·69e+09
	400	3·5	3·91e+04	7·91e+09
	800	11·8	7·44e+05	4·5e+10
	800	15·2	1·24e+06	5·83e+10
	1700	30·1	7·90e+05	1·88e+10
ST2040	crush	20·9	8·23e+05	2·81e+10
	400	2·9	7·65e+04	1·86e+10
	800	9·9	9·49e+05	6·86e+10
	1700	14·5	2·62e+05	1·29e+10

Noble gas data

Helium data are shown in Table IV. ^{3}He/^{4}He ratios reported here range from 1 to 123 R/R_a for individual heating steps (R_a is $(^3\text{He}/^4\text{He})_{\text{atmospheric}}$ and R is the measured (^{3}He/^{4}He); R_a=1·384×10^{-6}). ^{3}He/^{4}He ratios in the crushed fractions varied from 18 to 23R/R_a. Olivines collected along the Hawaiian Island chain and analysed by Rison and Craig (1983) have a range from 8 to 32R/R_a, with a ratio of 24R/R_a measured in olivine from the Napali member flows on Kauai. The Kauai values reported here are similar both to these, as well as to the range of 20 to 800 R/R_a presented in Kurz *et al.* (1990) and to the larger range of 5 to 2600 R/R_a detailed in Kurz (1986a) for olivines from young Hawaiian lava flows.

Helium release data are listed in Table IV. All the samples in which helium was measured were crushed on-line. Samples K560A and K560B correspond to helium measurements made on different aliquots from the same sample. K560A consisted of 1–2 mm sized grains, whereas K560B consisted of 0·5–0·25 mm sized grains. The release patterns varied between K560A and K560B. When the larger grains were analysed, the bulk of the ^{3}He atoms were released during the 1700°C step. When the smaller grains were analysed, the ^{3}He atoms were released principally during the crush, 800°C and 1700°C steps. Most of the ^{3}He was released from sample L600 during the two 800°C and one 1700°C steps, whereas the ^{3}He was released from ST2040 during the crush and 800°C steps.

Exposure ages based on the helium data were calculated assuming a value for the ^{3}He production rate at sea level of 100 atoms g^{-1} a^{-1}, as reported by Kurz (1986b), and were corrected for sample latitude and altitude (Lal, 1988). Because it was difficult to determine the spallation component in the helium analyses, we did not calculate a single exposure age based on the ^{3}He concentration data. Instead, we bracketed the possible exposure age. We calculated a range of apparent exposure ages: (1) a maximum age, or upper limit, was estimated by assuming all the ^{3}He measured in the samples to be cosmogenic and was calculated by dividing the total number of ^{3}He atoms measured by the production rate; (2) a minimum age or lower limit was estimated by assuming that only the ^{3}He released during temperature steps with a R/R_a ratio of greater than 20 was cosmogenic; and (3) a probable age was calculated assuming that only the ^{3}He atoms released during the final two temperature extractions in each run were cosmogenically produced. The probable age assumes that the cosmogenic component is released from the grains during heating, while the trapped component is assumed to be released during crushing (Kurz, 1986a). Representative age ranges are shown in Figure 5.

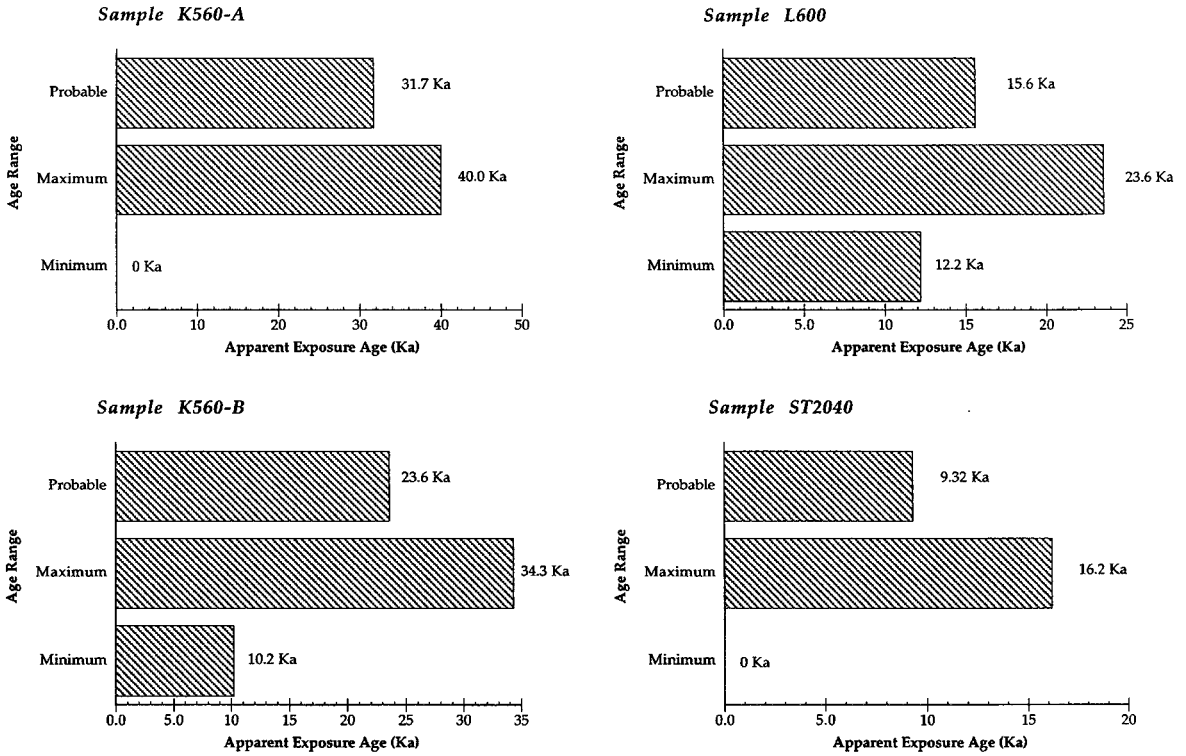

Figure 5. Representative ranges in exposure ages based on helium data. The probable, minimum and maximum ages are shown for four analyses.

Table V. ^{21}Ne data

Sample	Temperature step (°C)	20/21	^{21}Ne (atoms g^{-1})	Excess ^{21}Ne* (atoms g^{-1})
K560-1	800	0·00449	16·6	5·9
	1550	0·00422	40·3	0·05
K560-2	800	0·00377	0·2	0·03
	1550	0·00377	7·2	1·7
K560-3	800	0·00393	4·6	1·2
	1550	0·00383	7·7	1·9
KCKPD	1100	0·00308	0·7	0·042
	1600	0·00308	2·0	0·12
	1600	0·00314	0·7	0·051
	1850	0·00309	0·7	0·042
KVBPT	850	0·00315	0·2	0·016
	1050	0·00341	0·5	0·073
	1250	0·00301	0	0·011
	1500	0·00323	0	0·0051

*Excess ^{21}Ne relative to air

Neon data are presented in Table V. The intrinsic neon was expected to have atmospheric ratios of $(^{21}Ne/^{20}Ne)_{atmospheric}$=0·00296 (after Marti and Craig, 1987). Only ^{20}Ne and ^{21}Ne values are reported because of difficulties associated with the measurement of ^{22}Ne. Three aliquots from the same sample were measured: K560-1 consisted of 1–2 mm sized uncrushed grains, whereas K560-2 and K560-3 consisted of powdered

material (crushed under a continuous flow of N_2). The release patterns shown in Table V indicate that the uncrushed sample had a higher 20/21 ratio during the first heating step and a greater number of ^{21}Ne atoms g^{-1} released, relative to the uncrushed samples. The number of atoms of ^{21}Ne released during the two temperature steps was similar for the uncrushed samples.

To calculate exposure ages from the neon data, we used the ^{21}Ne production rate reported in Poreda and Cerling (1992), corrected for sample latitude and altitude (after Lal, 1988). Because we do not have ^{22}Ne data, we calculated maximum exposure ages from the 21/20 ratios by assuming all excess ^{21}Ne, relative to atmospheric values, to be cosmogenically produced. The basalts are young enough to disregard nucleogenic production of ^{21}Ne by $^{18}O(\alpha,n)$ (Kyser and Rison, 1982).

DISCUSSION

Comparison of radionuclide and noble gas exposure ages

Surface exposure ages calculated by measuring isotopes are shown in Table VI. Comparison of the data indicates inconsistencies between ages determined for the same samples using different isotopes. These inconsistencies raise several questions and may have implications for the retention of noble gases within the olivine crystals.

Table VI. Surface exposure ages

Sample	Isotope	Exposure age (ka)
K560	^{10}Be	186 (±21)
	^{26}Al	<119*
	^{3}He	0–40·0
	^{21}Ne	<160
	^{36}Cl	45·1 (±9)
	'Best age'	186 (±21)
KCKPD	^{26}Al	<20*
	^{21}Ne	<7
	^{36}Cl	49·3 (±10)
	'Best age'	<20*
KVBPT	^{26}Al	<70*
	^{21}Ne	<2
	^{36}Cl	56·8 (±11)
	'Best age'	<70*
L600	^{26}Al	38 (±10)
	^{3}He	12·2–23·6
	^{36}Cl	57·6 (±12)
	'Best age'	38 (±10)
ST2040	^{3}He	0–16·2
R900	^{26}Al	<2*
L-900-T	^{26}Al	<36*
L-900-S	^{26}Al	<31*
R-1600	^{26}Al	<17*
KKP1	^{26}Al	<24*
C2000	^{26}Al	<200*

*^{26}Al ages based on ^{26}Al concentration data quoted as the upper limit at two standard deviations

All five isotopes were measured in sample K560: the ^{10}Be-based age is 186 (±21)ka; the maximum age based on ^{21}Ne data is 160ka; the upper limit ^{26}Al data imply a maximum age of 119ka; the ^{36}Cl data indicate a 45ka age; whereas the ^{3}He data indicate a 32ka age.

The oldest age for sample K560 is based on the ^{10}Be datum. It is possible that this age is real and that the boulder has been exposed for over a 100ka. Alternatively, we may not have been successful in removing all the meteoric ^{10}Be from the surfaces of the grains. Future experiments will be designed to assess this. It is interesting to note, however, that the same etching technique was used successfully by Shepard *et al.* (1955) and that the ^{10}Be concentrations were constant in the final three leach fractions.

The ^{26}Al data are all quoted as upper limits at two standard deviations. The primary reason for the large uncertainty in the data is the high concentration of stable ^{27}Al in the olivines. Additional measurement to determine the range of ^{27}Al in olivines will allow estimation of the feasibility of measuring ^{26}Al in many olivine samples.

The ^{36}Cl data result in younger ages, relative to the ^{10}Be data, and both younger and older ages relative to the ^{26}Al upper limit data. In two of the samples, the ^{36}Cl ages are older than the upper limits based on the ^{26}Al data, whereas the ^{36}Cl ages are younger than the ^{26}Al upper limits for the other two samples. In general, it is interesting to note that all the ^{36}Cl-derived exposure ages cluster around 50ka. The low Cl content of the basalts could introduce error.

Other investigators have observed helium loss in quartz samples relative to ^{10}Be and ^{26}Al concentrations (e.g. Brook *et al.*, 1993). One of our goals was to determine whether ^{3}He and ^{21}Ne are quantitatively retained in olivines. Our initial result indicate a deficit of ^{3}He relative to ^{10}Be, ^{26}Al and ^{21}Ne, and it is tempting to say that there has been diffusive loss of cosmogenic ^{3}He relative to the other isotopes. In addition, an excess of ^{21}Ne relative to that expected was released at the lower (800°C) temperature steps. Comparison of the release patterns and amounts between crushed and uncrushed samples may imply possible loss post-crushing.

In his investigation of olivines from 0·5 Ma basalt flows, Kurz (1986a, b) saw no diffusive loss. However, Staudacher and Allegre (1991) noted lower ^{3}He concentrations in olivines derived from 30–40 Ma tuff deposits relative to the ^{21}Ne concentration measured. Cerling (1990) measured helium concentrations in olivines derived from <1 Ma flows and reported lower ^{3}He concentrations relative to what was expected based on K–Ar data. The difference was attributed to enhanced erosion rates in the past. However, increased erosion may not account for the discrepancies between expected and measured ^{3}He concentrations in weathered olivines. The noble gas results for the olivines reported in this paper are also derived from olivines emplaced in old (5·2 Ma) basalts. It is possible that over the course of millions of years, the olivines are changed structurally due to weathering, perhaps causing diffusive loss and migration of elements (noble gases) to fluid inclusion sites. Of course, it is not the absolute age of the olivine that matters, but rather its 'weathering age', which is related to the nature of the weathering environment. It may be that there is a weathering threshold which, when crossed, results in diffusive loss and migration of noble gases. The data presented here are too preliminary to unequivocally test this hypothesis, but seem to warrant further measurement of noble gases in olivines from rocks of varying age.

Geomorphic implications of exposure ages

Of the exposure ages presented in Table VI, we have chosen a 'best age' estimate or 'best limit age' for each of the samples. These ages are plotted along the Kaulaula Valley longitudinal profile in Figure 6. Boulder ages below the knickpoint range from 186ka to <2ka. The <2ka age for one of the boulders is difficult to explain; the boulder was neither resampled nor reanalysed. Downstream of the knickpoint, boulder exposure ages generally increase towards the coast. These data are generally consistent with the model for knickpoint propagation. The old boulder ages suggest that boulder mantling inhibits incision, implying that the channel downcutting rate is set both by weathering, breakdown and transport of boulders, and perhaps by knickpoint propagation under the boulder armour. The surprisingly slow rate of breakdown in a tropical environment points to the importance of knickpoint propagation. Old boulder ages further suggest little net sediment production in the last 200ka.

The age of the bedrock surface downstream and around the corner from the waterfall is <24ka based on the ^{26}Al data. Assuming 10m of waterfall retreat to have occurred over this upper limit of 24ka results in a waterfall retreat rate of approximately 0·4 mm a^{-1} can be calculated. These values bracket the approximate retreat rate of 1mm a^{-1}, calculated by assuming the knickpoint to have propagated 4km over 4Ma (Seidl *et al.*, 1994).

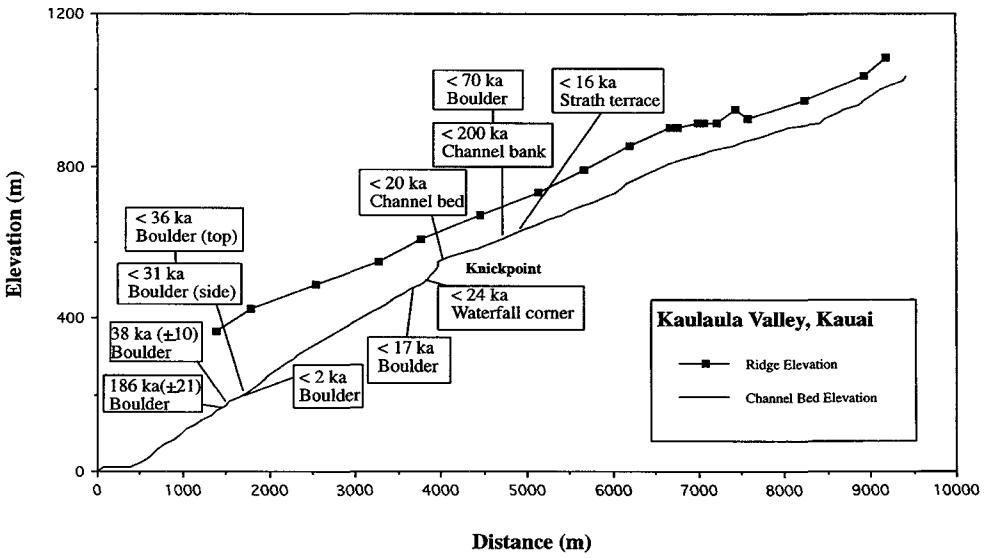

Figure 6. Surface exposure ages plotted on longitudinal profile of Kaulaula Valley. 'Best ages', as listed in Table VI and discussed in the text, are shown.

Upstream of the waterfall, the exposure age of the channel bed is <20 ka according to ^{26}Al. Lowering rates determined for sites upstream of the knickpoint are similar to long-term average rates determined based on the age of the rocks and the depth of the valley (Seidl *et al.*, 1994). The channel bank sample (C2000) was collected upstream of the waterfall at a site 2 m above the channel bed. Using the observed 2 m of bedrock channel incision at the site and the exposure age of <200 ka based on the upper limit ^{26}Al data implies a maxumum local erosion rate of roughly 0·01 mm a^{-1}. This estimate is the same order of magnitude as the average long-term erosion rate calculated for this site of 0·02 mm a^{-1}, based again on the known age of the rocks and the known depth of the valley (Seidl *et al.*, 1994). It is curious that the age of the well-rounded, small boulder sampled upstream of the knickpoint (KVBPT) is indistinguishable from the channel bank sample, yet is perched upon a pedestal of weathered bedrock.

CONCLUSIONS

^{10}Be, ^{26}Al, ^{36}Cl, ^{3}He and ^{21}Ne concentrations have been measured in several Kauai olivine samples using mass spectrometric and AMS techniques. Comparison of the data has pointed out some of the problems associated with measurement of multiple isotopes in olivine samples. Future work will focus on resolving and understanding the disparities between the different isotope concentrations. In particular, the possible diffusive loss of ^{3}He from the old olivines and the potential migration of ^{21}Ne within olivine crystals will be examined. From the geomorphic perspective, the calculated surface exposure ages are consistent with the knickpoint propagation hypothesis, and migration rates estimated from the isotopic data are similar to long-term estimates for the basin.

ACKNOWLEDGEMENTS

This work was funded by LLNL-IGPP grants nos 92-10 and 93-34 and by a Dissertation Fellowship from the American Association of University Women. We thank A. Howard, J. Kirchner, M. Power, N. Shubin and R.

Torres for enthusiastic field support and thoughtful discussions. We gratefully acknowledge the technical assistance of V. J. Brown, J. Koening and L. Harris. This work was partially supported under the auspices of the DOE by LLNL under contract W-7405-Eng-48.

REFERENCES

Bierman, P. 1994. 'Using in situ produced cosmogenic isotopes to estimate rates of landscape evolution: A review from the geomorphic perspective', *Journal of Geophysical Research*, **99**, 13 885–13 896.

Bierman, P. R. and Steig, E. J. 1996. 'Estimating rates of denudation using cosmogenic isotope abundances in sediments', *Earth Surface Processes and Landforms*, **21**, 125–139.

Bierman, P. R., Gillespie, A. R. and Caffee, M. W. 1995. 'Cosmogenic ages for earthquake recurrence intervals and debris flow fan deposition, Owens Valley, California', *Science*, **270**, 447–450.

Brook, E. J., Kurz, M. D., Ackert, R. P. Jr, Denton, G. H., Brown, E. T., Raisbeck, G. M. and Yiou, F. 1993. 'Chronology of Taylor Glacier advances in Arena Valley, Antarctica, using in situ cosmogenic ^{3}He and ^{10}Be'. *Quaternary Research*, **39**, 11–23.

Brown, E. T. and Gangue, ?. ?. 1995. 'Denudation rates determined from the accumulation of in situ-produced ^{10}Be in the Luquillo experimental forest, Puerto Rico', *Earth and Planetary Science Letters*, **129**, 193–202.

Brown, E. T., Bourles, D. L., Colin, F., Sanfo, Z., Raisbeck, G. M. and Yiou, F. 1994. 'The development of iron crust lateritic systems in Burkina Faso, West Africa examined with in-situ-produced cosmogenic nuclides', *Earth and Planetary Science Letters*, **124**, 19–33.

Burbank, D. W., Leland, J., Fielding, E., Anderson, R. S., Brozovic, N., Reid, M. R. and Duncan, C. 1996. 'Bedrock incision, rock uplift and threshold hillslopes in the northwestern Himalayas', *Nature*, **379**, 505–510.

Cerling, T. E. 1990. 'Dating of geomorphic surfaces using cosmogenic ^{3}He', *Quaternary Research*, **33**, 148–156.

Cerling, T. E. and Craig, H. 1994. 'Geomorphology and in-situ cosmogenic isotopes', *Annual Reviews of Earth and Planetary Science Letters*, **22**, 1273–1317.

Clague, D. A. and Dalrymple, G. B. 1987. 'The Hawaiian-Emperor Volcanic Chain Part I geologic evolution', in Decker, R. W., Wright, T. L. and Stauffer, P. H. (eds), *Volcanism in Hawaii*, US Geological Survey Professional Paper, **1350**, 5–54.

Craig, H. and Poreda, R. 1986. 'Cosmogenic ^{3}He in terrestrial rocks: the summit lavas of Maui', *Proceedings of the National Academy of Sciences*, **83**, 1970–1974.

Gosse, J. C., Klein, J., Evenson, E. B., Lawn, B. and Middleton, R. 1995. 'Beryllium-10 dating of the duration and retreat of the last Pinedale glacial sequence', *Science*, **268**, 1329–1333.

Granger, D., Kirchner, J. K. and Finkel, R. 1996. 'Spatially averaged long-term erosion rates from *in-situ* produced cosmogenic nuclides in sediments', *Journal of Geology*, **104**, 249–257.

Howard, A. D., Dietrich, W. E. and Seidl, M. A. 1994. 'Modeling fluvial erosion on regional to continental scales', *Journal of Geophysical Research*, **99**, 13 971–13 986.

Ivy-Ochs, S., Schluchter, C., Kubik, P. W., Dittrich-Hannen, B. and Beer J. 1995. 'Minimum ^{10}Be exposure ages of early Pliocene for the Table Mountain plateau and the Sirius Group at Mount Fleming, Dry Valleys, Antarctica', *Geology*, **23**, 1007–1010.

Kohl, C. P. and Nishiizumi, K. 1992. 'Chemical isolation of quartz for measurement of in-situ-produced cosmogenic nuclides', *Geochimica et Cosmochimica Acta*, **56**, 3583–3587.

Kurz, M. D. 1986a. 'Cosmogenic helium in a terrestrial igneous rock', *Nature*, **320**, 435–439.

Kurz, M. D. 1986b. '*In situ* production of terrestrial cosmogenic helium and some applications to geochronology', *Geochimica et Cosmochimica Acta*, **50**, 2855–2862.

Kurz, M. D., Colodner, D., Trull, T. W., Moore, R. B. and O'Brien, K. 1990. 'Cosmic ray exposure dating with in situ produced cosmogenic ^{3}He: Results from young Hawaiian flows', *Earth and Planetary Science Letters*, **97**, 177–189.

Kyser, T. K. and Rison, W. 1982. 'Systematics of rare gas isotopes in basic lavas and ultramafic xenoliths', *Journal of Geophysical Research*, **87**, 5611–5630.

Lal, D. 1988. 'In situ-produced cosmogenic isotopes in terrestrial rocks', *Annual Reviews in Earth and Planetary Sciences*, **16**, 355–388.

Lal, D. 1991. 'Cosmic ray labeling of erosion surfaces: In situ nuclide production rates and erosion models', *Earth and Planetary Science Letters*, **104**, 424–439.

Marti, K. and Craig, H. 1987. 'Cosmic-ray-produced neon and helium in the summit lavas of Maui', *Nature*, **325**, 335–337.

McKean, J.A., Dietrich, W.E., Finkel, R.C., Southon, J.R. and Caffee, M.W. 1993. 'Quantification of soil production and downslope creep rates from cosmogenic ^{10}Be accumulations on a hillslope profile', *Geology*, **21**, 343–346.

Monaghan, M. C., McKean, J., Dietrich, W. and Klein, J. 1992. '^{10}Be chronometry of bedrock-to-soil conversion rates', *Earth and Planetary Science Letters*, **111**, 483–492.

Nishiizumi, K., Winterer, E. L., Kohl, C. P., Klein, J., Middleton, R., Lal, D. and Arnold, J. R. 1989. 'Cosmic ray production rates of ^{10}Be and ^{26}Al in quartz from glacially polished rocks', *Journal of Geophysical Research*, **94**, 17 907–17 915.

Nishiizumi, K., Klein, J., Middleton, R. and Craig, H. 1990. 'Cosmogenic ^{10}Be, ^{26}Al, and ^{3}He in olivine from Maui lavas', *Earth and Planetary Science Letters*, **98**, 263–266.

Nishiizumi, K., Kohl, C. P., Arnold, J. R., Klein, J., Fink, D. and Middleton, R. 1991. 'Cosmic ray produced ^{10}Be and ^{26}Al in Antarctic rocks: Exposure and erosion history', *Earth and Planetary Science Letters*, **104**, 440–454.

Phillips, F. M., Zreda, M. G., Smith, S. S., Elmore, D., Kubik, P. W. and Sharma, P. 1990. 'Cosmogenic Chlorine-36 chronology for glacial deposits at Bloody Canyon, Eastern Sierra Nevada', *Science*, **248**, 1529–1532.

Poreda, R. J. and Cerling, T. E. 1992. 'Cosmogenic neon in recent lavas from the western United States', *Geophysical Research Letters*, **19**, 1863–1866.

Rison, W. and Craig, H. 1983. 'Helium isotopes and mantle volatiles in Loihi Seamount and Hawaiian Island basalts and xenoliths', *Earth and Planetary Science Letters*, **66**, 407–426.

Ritz, J. F., Brown, E. T., Bourles, D. L., Philip, H., Schlupp, A., Raisbeck, G. M., Yiou, F. and Enkhtuvshin, B. 1995. 'Slip rates along active faults estimated with cosmic-ray-exposure dates: Application to the Bogd fault, Gobi-Altai, Mongolia', *Geology*, **23**, 1019–1022.

Seidl, M. A. 1993. *Form and process in channel incision of bedrock*, PhD Thesis, University of California at Berkeley, 163 pp.
Seidl, M. A. and Dietrich, W. E. 1992. 'The problem of bedrock channel erosion', in Schmidt, K.-H. and De Ploey, J. (Eds), *Functional Geomorphology: Landform Analysis and Models: Catena Supplement*, **23**, 101–124.
Seidl, M. A., Dietrich, W. E. and Kirchner, J. K. 1994. 'Longitudinal profile development into bedrock: An analysis of Hawaiian channels', *Journal of Geology*, **102**, 457–474.
Shepard, M. K., Arvidson, R. E., Caffee, M., Finkel, R. and Harris, L. 1995. Cosmogenic exposure ages of basalt flows: Lunar Crater volcanic field, Nevada', *Geology*, **23**, 21–24.
Staudacher, T. and Allegre, C. J. 1991. 'Cosmogenic neon in ultramafic nodules from Asia and in quartzite from Antarctica', *Earth and Planetary Science Letters*, **106**, 87–102.
Stearns, H. T. 1985. *Geology of the State of Hawaii*, Pacific Books, Palo Alto, 335.
Zreda, M. G., Phillips, F. M., Elmore, D., Kubik, P. W., Sharma, P. and Dorn, R. I. 1991. 'Cosmogenic ^{36}Cl production rates in terrestrial rocks', *Earth and Planetary Science Letters*, **105**, 94–109.
Zreda, M. G., Phillips, F. M., Kubik, P. W., Sharma, P. and Elmore, D. 1993. 'Cosmogenic ^{36}Cl dating of a young basaltic eruption complex, Lathrop Wells, Nevada', *Geology*, **21**, 57–60.